CORA Cork Open Research Archive
Cartlann Taighde Oscailte Chorcaí

Title	Functionalization of SiO2 surfaces for Si monolayer doping with minimal carbon contamination
Authors	van Druenen, Maart;Collins, Gillian;Glynn, Colm;O'Dwyer, Colm;Holmes, Justin D.
Publication date	2017-12-14
Original Citation	van Druenen, M., Collins, G., Glynn, C., O'Dwyer, C. and Holmes, J. D. (2018) 'Functionalization of SiO2 Surfaces for Si Monolayer Doping with Minimal Carbon Contamination', ACS Applied Materials & Interfaces, 10(2), pp. 2191-2201. doi:10.1021/acsami.7b16950
Type of publication	Article (peer-reviewed)
Link to publisher's version	https://pubs.acs.org/doi/10.1021/acsami.7b16950 - 10.1021/acsami.7b16950
Rights	© 2017 American Chemical Society. This document is the Accepted Manuscript version of a Published Work that appeared in final form in ACS Applied Materials and Interfaces, copyright © American Chemical Society after peer review and technical editing by the publisher. To access the final edited and published work see http://pubs.acs.org/doi/pdf/10.1021/acsami.7b16950
Download date	2025-03-21 23:04:11
Item downloaded from	https://hdl.handle.net/10468/5251

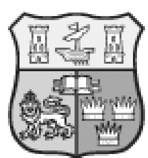

UCC
University College Cork, Ireland
Coláiste na hOllscoile Corcaigh

ACS APPLIED MATERIALS & INTERFACES

Subscriber access provided by UNIV COLL CORK

Article

Functionalization of SiO Surfaces for Si Monolayer Doping with Minimal Carbon Contamination

Maart van Dreunen, Gillian Collins, Colm Glynn, Colm O'Dwyer, and Justin D. Holmes

ACS Appl. Mater. Interfaces, **Just Accepted Manuscript** • DOI: 10.1021/acsami.7b16950 • Publication Date (Web): 14 Dec 2017

Downloaded from http://pubs.acs.org on December 20, 2017

Just Accepted

"Just Accepted" manuscripts have been peer-reviewed and accepted for publication. They are posted online prior to technical editing, formatting for publication and author proofing. The American Chemical Society provides "Just Accepted" as a free service to the research community to expedite the dissemination of scientific material as soon as possible after acceptance. "Just Accepted" manuscripts appear in full in PDF format accompanied by an HTML abstract. "Just Accepted" manuscripts have been fully peer reviewed, but should not be considered the official version of record. They are accessible to all readers and citable by the Digital Object Identifier (DOI®). "Just Accepted" is an optional service offered to authors. Therefore, the "Just Accepted" Web site may not include all articles that will be published in the journal. After a manuscript is technically edited and formatted, it will be removed from the "Just Accepted" Web site and published as an ASAP article. Note that technical editing may introduce minor changes to the manuscript text and/or graphics which could affect content, and all legal disclaimers and ethical guidelines that apply to the journal pertain. ACS cannot be held responsible for errors or consequences arising from the use of information contained in these "Just Accepted" manuscripts.

ACS Publications

ACS Applied Materials & Interfaces is published by the American Chemical Society.
1155 Sixteenth Street N.W., Washington, DC 20036
Published by American Chemical Society. Copyright © American Chemical Society.
However, no copyright claim is made to original U.S. Government works, or works produced by employees of any Commonwealth realm Crown government in the course of their duties.

1
2
3
4
5
6
7
8
9
10
11
12
13
14
15
16
17
18
19
20
21
22
23
24
25
26
27
28
29
30
31
32
33
34
35
36
37
38
39
40
41
42
43
44
45
46
47
48
49
50
51
52
53
54
55
56
57
58
59
60

Functionalization of SiO_2 Surfaces for Si Monolayer Doping with Minimal Carbon Contamination

Maart van Druenen[1, 2], Gillian Collins[1, 2 *], Colm Glynn[1], Colm O'Dwyer[1] and Justin D. Holmes[1, 2]

[1]*School of Chemistry, University College Cork, Ireland.*

[2]*CRANN@AMBER, Trinity College Dublin, Dublin 2, Ireland.*

*To whom correspondence should be addressed: Tel: +353 (0)21 4905143; E-mail: g.collins@ucc.ie

Keywords: monolayer, doping, silicon, covalent functionalization, phosphonic acids, X-ray photoelectron spectroscopy, stability, carbon contamination

Abstract

Monolayer Doping (MLD) involves the functionalization of semiconductor surfaces followed by an annealing step to diffuse the dopant into the substrate. We report an alternative doping method, oxide-MLD, where ultra-thin SiO_2 overlayers are functionalized with phosphonic acids for doping Si. Similar peak carrier concentrations were achieved when compared to hydrosilylated surfaces (~2×10^{20} atoms/cm^3). Oxide-MLD offers several advantages over conventional MLD such as ease of sample processing, superior ambient stability and minimal carbon contamination. The incorporation of an oxide layer minimizes carbon contamination by facilitating attachment of carbon-free precursors or by impeding carbon diffusion. The oxide-MLD strategy allows selection of many inexpensive precursors and therefore allows application

to both p- and n-doping. The phosphonic acid functionalized SiO_2 surfaces were investigated using XPS and ATR-FTIR spectroscopy while doping was assessed using electrochemical capacitance voltage and Hall measurements.

Introduction

The doping of nanostructures is becoming increasingly difficult due to the rapid down scaling of device dimensions. A doping technique recently developed to keep up with device scaling is monolayer doping (MLD), which involves the functionalization of a semiconductor surface followed by an annealing step to drive the dopant into the substrate[1]. Current doping techniques, such as ion implantation, often lead to crystal damage, are incompatible with nanostructures and suffer from a lack of control in forming shallow junctions[2]. MLD has been reported to be compatible with nanostructures, a variety of semiconductor surfaces and allows tailoring of dopant dose[3,4,5,6,7]. Controlled doping with increased precision of dopant atom placement can be achieved due to the incorporation of a surface functionalization step allowing application to 3D structures[8, 9]. In addition, MLD is a damage-free method that shows promise in achieving ultra-shallow junctions allowing it to keep up with scaling device dimensions[10]. A more detailed summary of current advances in doping techniques has been reported elsewhere[11].

MLD has been studied extensively on Si surfaces due to its importance for device applications. The functionalization of the semiconductor surface has proven to be an advantage of MLD in achieving uniform doping in 3D architectures, such as nanowires, which is more challenging to achieve using conventional doping techniques such as ion implantation[3]. The preferred method for surface functionalization on Si for MLD is hydrosilylation, where a precursor containing a

dopant atom and an alkene functional group reacts with a hydride-terminated Si surface[12,13]. However, hydrosilylation of Si surfaces is air and moisture sensitive, requiring rigorous purification of solvents and precursors. The functionalized surfaces also have limited ambient stability before re-oxidation of the surface.

MLD of Si by functionalizing the native SiO_2, first reported by Mathey *et al.* [14] and Alphazan *et al.* [15], typically employ silanol dopant precursors that act as both a dopant source and a capping layer for Si MLD. Capping layers are used to prevent dopant evaporation during the rapid thermal anneal (RTA). Employing a self-capping precursor that has been designed to prevent phosphorus evaporation ensures the dopant atoms preferentially enter the Si substrate while releasing the precursor ligands and minimizing carbon contamination. [14,15] In this manuscript, we describe how MLD can be achieved through functionalization of an ultra-thin SiO_2 overlayer using simple phosphonic acids[16]. Significantly, we compare MLD using hydrosilylation with SiO_2 functionalization and demonstrate similar peak carrier concentrations can be achieved for both strategies ($\sim 2 \times 10^{20}$ atoms/cm^3). Advantages of this approach include compatibility with ambient conditions and no drying of solvents or precursors. MLD via oxide functionalization is applicable to a wide range of inexpensive and commercially available precursors. As reported by Vega *et al.* [17] phosphonic acids initially physisorb on the SiO_2 surface and a thermal anneal initiates covalent bond formation[17]. Due to the presence of the SiO_2 layer and the superior passivation properties of phosphonic acids, these surfaces display increased stability compared to hydrosilylated surfaces and do not result in uncontrollable re-oxidation of the Si surface, which often occurs during a thermal hydrosilylation reaction[18]. The use of phosphonic acids allows selection of low-carbon or non-carbon containing precursors, hence avoiding carbon

contamination. More importantly the oxide layer provides a barrier to carbon contamination, which is a key challenge for MLD. Carbon has been reported to segregate at the Si-SiO_2 interface while remaining at the SiO_2 side, allowing it to be removed using HF treatment and ensuring minimal carbon contamination[19].

We have investigated the oxide functionalization process in detail using X-ray photoelectron spectroscopy (XPS), attenuated total reflectance infrared spectroscopy (ATR-FTIR), water contact angle (CA), electrochemical capacitance voltage measurements (ECV) and secondary ion mass spectrometry (SIMS) in comparison with hydrosilylated surfaces in terms of ease of functionalization strategy, stability and doping concentration. The use of physisorbed phosphonic acid layers has also been investigated as a doping strategy, a method comparable to spin-on-doping[20]. We demonstrate that carbon contamination is minimal using this oxide-MLD approach. Furthermore, the effect of carbon contamination can be avoided as carbon-free precursors can be used with oxide-MLD.

Experimental

Sulfuric acid (95-97 %), hydrogen peroxide (30 % w/w), nitric acid (64-66 %), ammonium hydroxide (30-33 %) and all other chemicals were purchased from Sigma-Aldrich. Glassware was cleaned using a Piranha solution followed by rinsing in water and stored overnight in a 140 °C oven.

1
2
3
4
5
6
7
8
9
10
11
12
13
14
15
16
17
18
19
20
21
22
23
24
25
26
27
28
29
30
31
32
33
34
35
36
37
38
39
40
41
42
43
44
45
46
47
48
49
50
51
52
53
54
55
56
57
58
59
60

Hydrosilylation

Functionalization of oxide-free surfaces was carried out using conventional hydrosilylation of H-terminated Si surfaces. Mesitylene (98 %) was dried overnight using CaH_2 (95 %) and distilled under reduced pressure onto molecular sieves (4 Å). Vinyl phosphonic acid (97 %) (VPA) was dried using P_2O_5 (99 %) and subsequently filtered through alumina onto molecular sieves. Diethylvinyl phosphonate (97 %) (DVP) was dried using CaH_2 and distilled under reduced pressure or dried using the same procedure as VPA. Substrates of 1 × 1 cm were cut from a (100) Si wafer and degreased by 2 min of sonication in IPA (99.9 %). A Piranha (3:1 H_2SO_4:H_2O_2) solution was used to clean the samples followed by copious rinsing with water. Oxide removal and H-termination was achieved using a 10 % HF (≥40 %) dip for 2 min. The samples were dried under a stream of nitrogen and placed in a 100 ml round-bottomed flask, previously cooled under an inert environment, under vacuum for 30 min (refilling with argon every 10 min). Ten freeze-pump thaw cycles were used to degas the precursor solution prior to use (0.13 mM for VPA, 0.5 mM for diethyl DVP). Optimal concentrations were determined using XPS analysis. The mixture was added to the reaction flask using cannula transfer and refluxed under argon at 160 °C for 2 h. After the reaction cooled to room temperature the samples were sonicated in anhydrous toluene (≥99.8 %) for 10 min with subsequent rinsing in anhydrous ethanol (≥99.5 %), anhydrous dichloromethane (≥99.8) (DCM) and toluene to remove physi-adsorbed material. Samples were stored under nitrogen to prevent oxidation before analysis took place.

1
2
3
4
5
6
7
8
9
10
11
12
13
14
15
16
17
18
19
20
21
22
23
24
25
26
27
28
29
30
31
32
33
34
35
36
37
38
39
40
41
42
43
44
45
46
47
48
49
50
51
52
53
54
55
56
57
58
59
60

Oxide Functionalization

Ultra-thin SiO_2 layers were prepared using conventional RCA cleaning procedures. Si substrates were degreased by sonicating in IPA for 2 min and cleaned using a Piranha solution. H-termination was achieved using a 5 % HF dip for 2 min followed by an RCA clean ($NH_4OH:H_2O_2:H_2O$ in a 1:1:5 ratio) to re-oxidize the surface for oxide functionalization. Samples were placed in a solution of the phosphonic acid dissolved in 10 ml of anhydrous THF (≥99.9 %) for 24 hr or a week to form a physisorbed self-assembled monolayer (SAM). The optimal phosphonic acid concentrations were determined by evaluating the WCA and XPS analysis of the functionalized surfaces (34 mM for VPA, 63 mM for phenylphosphonic acid (98 %) (PPA), 8 mM for n-dodecylphosphosphonic acid (≥89.5 %) (DPA), 12 mM for 1H,1H,2H,2H–perfluorooctanephosphonic acid (95 %) (FOPA), 12 mM for octadecylphosphonic acid (97 %) (OPA), 80 mM for boric acid (≥99.5 %) (BA), a 25 mM phenylboronic acid (≥97 %) (PBA)). A carbon-free precursor, phosphorus pentoxide (P_2O_5), was also used with two different concentrations: 7 mM and 14 mM. The substrates were removed from solution and dried under a stream of nitrogen before annealing at 140 °C for 1 or 24 hr in an ambient environment (oven) or moisture-free environment (vacuum oven or on Schlenk line under argon). Following annealing, physisorbed material was removed using one of two rinses: sonication in THF and then ethanol for 10 min each or sonication in a base rinse (10:3:1 water: THF: trimethylamine (99 %)) and ethanol for 10 min each. Samples were stores under nitrogen before analysis was carried out.

Oxide Growth for Oxide Spacer of Different Thicknesses

A previously published procedure was used to electrochemically and chemically grow thin oxide layers (5-20 nm) on Si in a 1M HNO_3 electrolyte[21]. Anodic oxidation occurred at the Si working

electrode (WE) with a Pt counter electrode (CE) and a calomel reference electrode with potentials of 10 to 20 V applied using a potentiostat or using only WE, CE and a power source to provide voltages greater than 10 V. Nitric acid oxidation of Si (NAOS) was employed to chemically grow oxide layers using a 40 wt. % solution of nitric acid which was heated to 108 °C for ~1.5 hr until the azeotropic point was reached[22]. After which the solution was added to a round-bottomed flask and refluxed at 121 °C for 14 hr.

Surface Characterization

X-Ray photoelectron spectroscopy (XPS) analysis was carried out on an Oxford Applied Research Escabase XPS system with a nonmonochromated Al Kα X-Ray source at 200 W with a base pressure of 5 x 10^{-10} mbar. Survey spectra were acquired at 0-1000 eV using a step size of 0.7 eV, a dwell time of 0.3 s and a pass energy of 100 eV. Core level scans were averaged over 20-40 scans at a step size of 0.1 eV, a dwell time of 0.1 s and a pass energy of 50 eV. Spectra were recorded normal to the surface direction and also at a grazing angle of 165 ° from the axis of recording. XPS was also carried out using a Kratos AXIS-ULTRA XPS using monochromated Al X-rays at 150 W. Survey spectra were recorded at a pass energy of 160 eV with a step size of 1 eV and a dwell time of 50 ms. Core level scans were acquired at 20 eV with a step size of 0.05 eV and a dwell time of 100 ms. These measurements were recorded normal to the surface direction. Scans were averaged over 12 scans for the survey scans and 5-40 for core level scans. CasaXPS software was used to process the spectra with Shirley background correction and peaks fitted to Voigt profiles. Peaks were charge corrected to the C 1s peak at 285 eV. SiO_2 thicknesses were calculated using the thickogram[23] and measurements were averaged over 3 samples. Attenuated total reflectance infrared (ATR-FTIR) spectra were

recorded using a Nicolet 6700 Infrared Spectrometer with a VariGATR and a liquid cooled MgCdTe detector using 3000 scans at a resolution of 2 cm^{-1}. Spectra were collected under p-polarization in an ambient atmosphere. ATR-FTIR spectra were also collected using a Bruker Platinum ATR using 1000 scans. Contact angle measurements were recorded using deionised water on a Data Physics Contact Angle instrument using a minimum of 8 measurements per sample.

Dopant Profiling

Samples were capped with 50 nm of sputtered SiO_2 and samples were placed in a rapid thermal anneal furnace for 5 seconds at 950, 1000, 1050 or 1100 °C. A WEP Control CVP21 Wafer Profiler was used for ECV analysis. A 0.1 M ammonium hydrogen difluoride (≥98.5 %) solution was used as an etchant. SIMS analysis was carried out on an ION TOF TOF-SIMS 5. Sputtering was carried out with a Cs^+ ion beam and analysis was completed using a 25 keV Bi^+ ion beam incident at 45° of a 40 µm × 40 µm area. ECV and SIMS measurements were carried out in duplicate and analysis displayed is an average of the two measurements. Hall Effect measurements were acquired using a LakeShore® 8600 series instrument, with an excitation field of 1.7 T and an excitation current from 10 µA to 100 µA. Errors in measurements can occur due to the approximation of samples to the van der Pauw geometry.

Results and Discussion

Comparison of Oxide with Oxide-free Functionalization

Si surfaces were covalently functionalized with the same precursor, vinylphosphonic acid (VPA), using two methods. Attachment of VPA occurred via the alkene group to H-terminated Si using hydrosilylation. VPA was also attached via the surface silanol groups on an ultra-thin

1 2 3 4 5 6 7 8 9 10 11 12 13 14 15 16 17 18 19 20 21 22 23 24 25 26 27 28 29 30 31 32 33 34 35 36 37 38 39 40 41 42 43 44 45 46 47 48 49 50 51 52 53 54 55 56 57 58 59 60

(0.4 nm) SiO_2 overlayer via a condensation reaction of the phosphonic acid and surface hydroxyl groups as shown in Figure 1. Surfaces functionalized by hydrosilylation displayed re-oxidation during the reaction, as illustrated by comparison of the Si 2p core level XPS in Figures 2(a) and (b). Under hydrosilylation conditions with VPA, oxide growth was estimated to be 0.5 nm, as determined by the appearance of an oxide shoulder at a binding energy of 103 eV. A variety of phosphonates and phosphonic acids were used for hydrosilylation reactions such as VPA, diethyl vinylphosphonate, allyldiphenylphosphine and allyldiphenylphosphine oxide. Si 2p spectra after the hydrosilylation reaction always displayed some degree of surface oxidation, as illustrated in figure 2(b). Air exposure of samples was minimal prior to XPS analysis, suggesting oxidation may have originated from the presence of trace water impurities in the precursors, as hydrosilylation using a non-hygroscopic precursor (1,7-dialkyne) used as a reference, resulted in an oxide-free surface. IR analysis of precursors showed a broad hydrogen-bonded OH peak at 3500 cm^{-1} due to water as shown in Figure S1, which was minimized after drying but complete removal of water may not be achieved due to strong H-bonding with the phosphonate or phosphonic acid group. In comparison, Si surfaces functionalized via the silanol group in the SiO_2 overlayer showed negligible changes in surface oxide thickness after functionalization, as shown in Figures 2(c) and (d). Minimal re-oxidation of the SiO_2 surface during the oxide functionalization reaction can be attributed to the more robust nature of the oxide functionalization process.

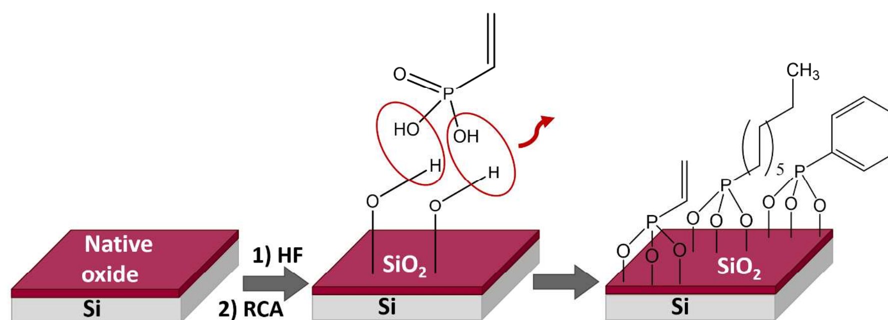

Figure 1: Reaction scheme illustrating the oxide functionalization process. A hydroxyl terminated surface is achieved using an RCA clean, which subsequently reacts in a condensation reaction with a range of phosphonic acids.

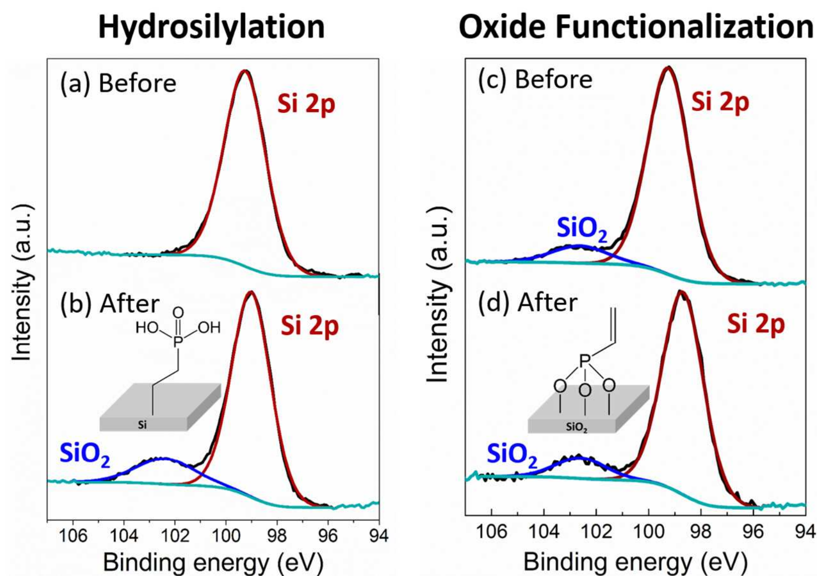

Figure 2: Si 2p peak for (a) H-terminated Si before hydrosilylation and (b) after a hydrosilylation reaction. SiO_2 terminated surface (c) before and (d) after functionalization.

Functionalization of an SiO_2 overlayer on Si with the dopant precursor was investigated to overcome the problems of functionalization via hydrosilylation and to develop an MLD doping strategy using inexpensive, widely available precursors, without the need for inert conditions and purification of solvents and precursors. Successful phosphonic acid functionalization was confirmed by the presence of the P 2s and P 2p XPS signals, with analysis being carried out after prolonged sonication in THF and ethanol to remove physisorbed species, hence ensuring these signals were predominantly associated with chemisorbed species. Due to the overlap of both P 2s and P 2p signals with Si 2s and Si 2p plasmons, additional XPS measurements were carried out at a grazing angle, enhancing surface sensitivity. Further details of angle resolved measurements are provided in Figure S2 (see Supporting Information). The XPS spectrum in Figure 3(a) represents the Si 2s plasmon overlapping with the P 2s peak acquired at the normal angle of analysis (0 °). Figure 3(b) shows the spectrum obtained at an angle of 75 ° where a clear reduction of the Si plasmon and an increase in the intensity of the phosphorus peak is illustrated proving its presence on the surface. Due to the overlap of P 2s and P 2p signals with Si plasmons, the attachment of phosphonic acids was further confirmed using 1H,1H,2H,2H–perfluorooctanephosphonic acid, which shows characteristic deconvoluted carbon environments due to the high electronegativity of F. The C 1s spectrum in Figure 3(c) displays the deconvoluted carbon environments. A peak at a B. E. of 293.9 eV attributed to the CF_3 group and a peak at 289.8 eV can be assigned to the CF_2 groups. The contribution at 286.4 eV corresponds to C-C-F, and C-O groups. Adventitious carbon is associated with the peak at a B. E. of 284.6 eV. Additionally, the F 1s peak at 689 eV shown in the inset in Figure 3(c) further confirmed surface attachment. The long term stability of oxide functionalized substrates was also assessed and compared to hydrosilylated samples using the Si 2p and P 2s core levels over a

period of 24 hours, a week and a month. Figure 3(d) compares the SiO_2:Si ratio for hydrosilylated and oxide functionalized substrates. No residual oxide growth was observed after a period of a month for oxide functionalized substrates when compared to a non-functionalized RCA cleaned wafer, demonstrating excellent ambient stability. When hydrosilylated samples were exposed to air, oxidation occurred within the first 24 hr. After one month of ambient exposure the oxide increased by 12.4 %. The P 2s peak for oxide functionalized samples displayed similar amounts of phosphorus were present after a month of exposure to ambient conditions, unlike hydrosilylated samples where a decrease in the P 2p peak was observed, indicating superior passivation properties of oxide functionalized surfaces.

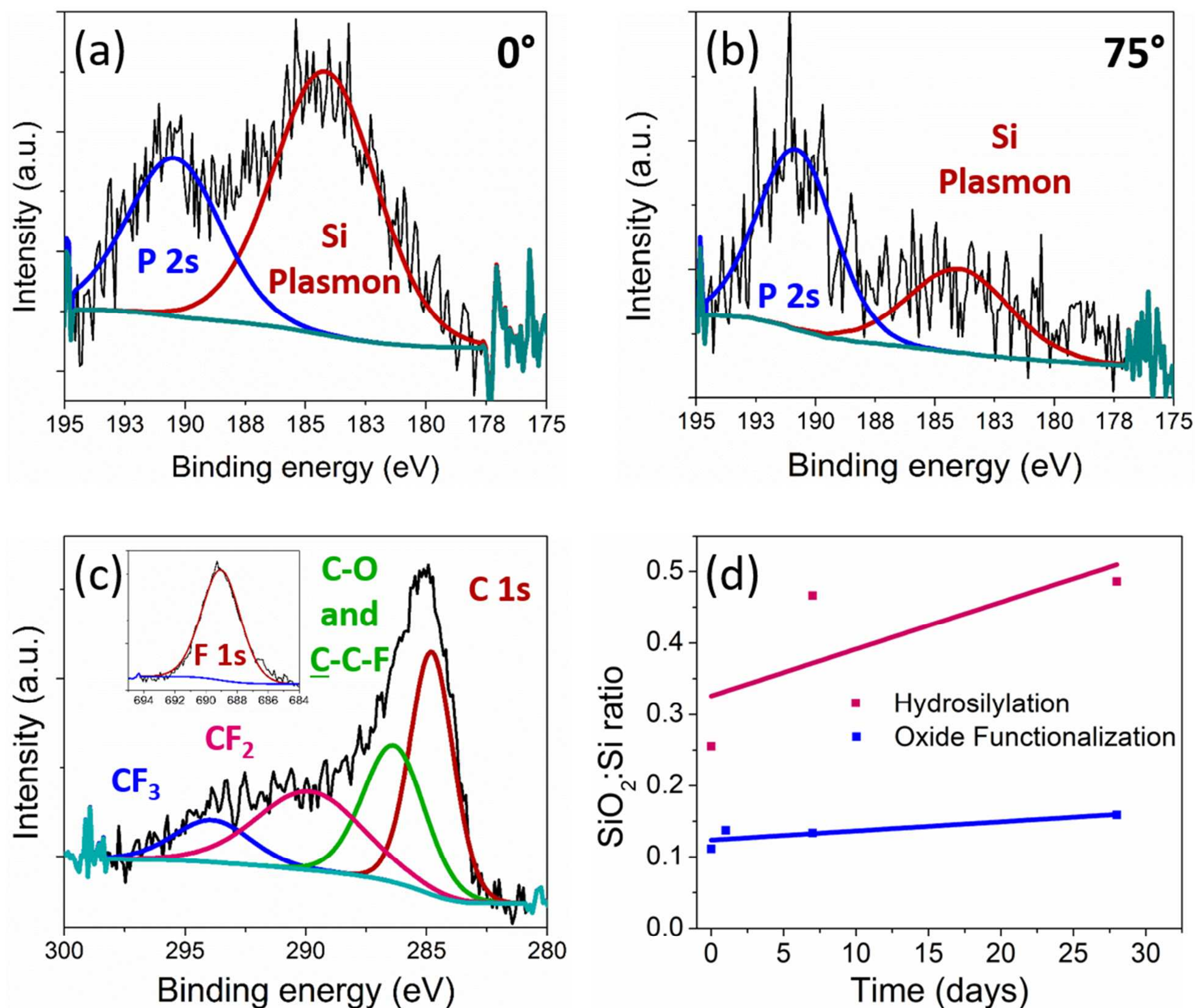

Figure 3: Surface attachment was confirmed using grazing angle XPS of VPA and a fluorinated phosphonic acid. a) The P 2s peak of a VPA functionalized SiO_2 surface was acquired at 0 ° while b) was acquired at 75 °. The C 1s peak of a FOPA functionalized SiO_2 surface is shown in c) where deconvoluted carbon environments are displayed with the inset showing the F 1s peak. d) The SiO_2:Si ratio as a function of time is depicted for both hydrosilylation and oxide functionalization.

1
2
3
4
5
6
7
8
9
10
11
12
13
14
15
16
17
18
19
20
21
22
23
24
25
26
27
28
29
30
31
32
33
34
35
36
37
38
39
40
41
42
43
44
45
46
47
48
49
50
51
52
53
54
55
56
57
58
59
60

Monolayer Optimization

Reproducibility of doping profiles is dependent on a monolayer coverage obtained through functionalization. Optimization of the oxide-MLD methodology was investigated using phenylphosphonic acid (PPA). Changes in the P 2s peak of a PPA functionalized SiO_2 surface were evaluated at different stages of the functionalization procedure to distinguish between physisorption and chemisorption. Figure S3 (see Supporting Information) compares the P 2s peak for PPA functionalized surfaces before annealing (pre-anneal), after annealing without rinsing (post-anneal) and after prolonged sonication (post-sonication). A shift of the P 2s binding energy from 191.4 eV for the pre-annealed to 190.8 eV for post-annealed sample, to 189 eV after sonication is consistent with the conversion of physisorbed phosphonic acid multilayers in the pre- and post-annealed samples to covalently bound phosphonic acid monolayers after sonication. The decrease in the P 2s binding energy is associated with the conversion of P-O-H bonds to P-O-Si bonds[24]. Formation of P-O-Si bonds can also be monitored by comparison of the O 1s peak at different stages as shown in Figures 4(a)-(c). The O 1s can be deconvoluted into the P=O component at a binding energy of ~534 eV, and the P-O-H component at ~531 eV. A broadening of the O 1s FWHM from 2.2 eV for the pre-anneal to 2.3 eV for the post-sonication substrate occurred due to the incorporation of a P-O-Si component in the main component of the O 1s peak[24]. The broadening of the O 1s peak and shift of the P 2s peak indicate chemisorption of phosphonic acids and removal of physisorbed species from the SiO_2 surface. The effect of different immersion times in the phosphonic acid solution were investigated to monitor the effect on surface coverage and further oxidation as the solution was exposed to air for the full duration of sample immersion. Longer immersion times (7 days compared to 24 hr) did not result in growth of the underlying oxide but also did not improve

1
2
3
4
5
6
7
8
9
10
11
12
13
14
15
16
17
18
19
20
21
22
23
24
25
26
27
28
29
30
31
32
33
34
35
36
37
38
39
40
41
42
43
44
45
46
47
48
49
50
51
52
53
54
55
56
57
58
59
60

surface coverage as indicated by similar intensities of the P 2s peaks. Once the thermodynamically stable SAM is formed it acts as a passivation layer that protects the surface from oxidation. The attachment of alkyl phosphonates (diethyl vinylphosphonate) on SiO_2 overlayers was also investigated using the same conditions employed for phosphonic acids but an increase in the oxide thickness from 0.4 nm to 1.3 nm was observed during functionalization. Growth in the oxide may be due to the bulky steric configuration of the ethyl side groups of the phosphonate molecule which hinders surface attachment leading to incomplete passivation of the oxide layer, consequently resulting in additional oxide growth during the anneal. Uniform phosphonate SAM formation has been reported to be highly dependent on the interaction between substituents such as H-bonding between surface hydroxyls and the phosphonate head group and π-π interactions between aryl substituents which can facilitate monolayer formation[25]. The additional oxide growth obtained using phosphonates suggests that phosphonic acids are more suitable for the functionalization of surface silanol groups due to their steric configuration which provides superior passivation.

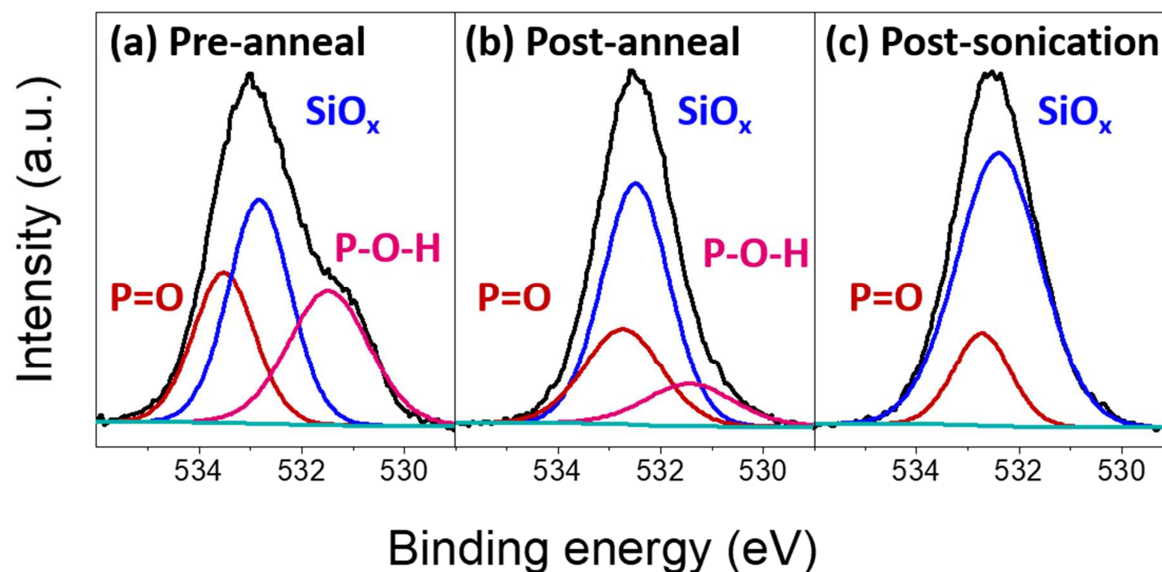

Figure 4: Surface analysis using the O 1s XPS peak to investigate the extent of chemisorption of phosphonic acids to the SiO_2 surface comparing (a) pre-anneal, (b) post-anneal and (c) post-sonication.

The annealing time was also found to influence oxide growth during the reaction. An anneal time of 24 hr[26,27,24,28] was used in preliminary experiments. This anneal time resulted in growth of the oxide layer and visible surface staining which could not be readily removed by sonication. In-situ IR analysis studied by Vega *et al.* [17] revealed that attachment of phosphonic acids to SiO_2 occurs within seconds of reaching 140 °C in a low humidity environment, while no attachment was observed when humidity levels exceeded 16 %[17]. Consequently, the effect of humidity during the anneal step was evaluated. When samples were annealed under standard humidity levels (oven at 140 º C), attachment was confirmed using the XPS P 2s peak but these samples lacked a P-O-Si peak when analyzed using ATR-FTIR. Annealing the samples under low humidity, either under nitrogen or in a vacuum oven, improved the surface coverage of chemisorbed species as indicated by the appearance of a peak at 1100 cm^{-1}, corresponding to P-

1
2
3
4
5
6
7
8
9
10
11
12
13
14
15
16
17
18
19
20
21
22
23
24
25
26
27
28
29
30
31
32
33
34
35
36
37
38
39
40
41
42
43
44
45
46
47
48
49
50
51
52
53
54
55
56
57
58
59
60

O-Si bond formation. Chemical attachment of phosphonic acids to SiO_2 surfaces is best achieved in low humidity environments, as the hydroxyl network must be broken for the surface to react[17]. The presence of P 2s peaks for samples annealed in air prove both annealing methods will result in successful functionalization, however, optimum coverage will be obtained when water is removed continuously which will drive the condensation reaction. The presence of a P-O-Si signal confirms covalent attachment of phosphonic acids to the SiO_2 surface. Additionally, the shift of the P 2s peak has previously been reported to be associated with monolayer coverage but the presence of physisorbed species has not been ruled out. Water contact angle measurements were carried out to assess the packing of phosphonic acids at the surface. Poorly formed monolayers and physisorbed species typically display lower contact angles compared to well order monolayers. Table S1 and Figure S4 (see Supporting Information) show the change in contact angle of 22 ° for an RCA cleaned SiO_2 surface to > 90 ° after functionalization indicating the successful formation of a hydrophobic monolayer.

Binding Mechanism of Surface Attachment of Phosphonic acids

The attachment of phosphonic acids to oxide surfaces has been well studied and their surface coordination can display three main binding modes: monodentate, bidentate, tridentate (displayed in Figure 5) or a combination of any mixture of these[17, 16, 24, 29-30]. The bonding mechanism of phosphonic acids and confirmation of a covalently bound monolayer was investigated using complementary XPS and ATR-FTIR by evaluating the surfaces at different stages during the functionalization process. Prior to annealing, the surface consists of a physisorbed overlayer (pre-anneal), which on annealing at 140 °C converts to a chemisorbed layer at the SiO_2 interface (post-anneal). Rinsing and sonication removes physisorbed

phosphonic acid species leaving a phosphonic acid monolayer covalently bound to the surface (post-sonication). Comparison of a pre-anneal substrate (with physisorbed species) to a post-anneal substrate (with both chemisorbed and physisorbed species) and to a post anneal and sonicated substrate (with only a chemisorbed monolayer) allows the mechanism of attachment to be probed.

Figures 5(a)-(c) illustrate the ATR-FTIR spectra of these 3 binding modes in the phosphonic acid absorption region. Figure 5(a) shows the pre-anneal substrate where symmetric P-O stretches were observed at 1025-975 cm^{-1} and asymmetric stretches at 1070 cm^{-1}, indicating the presence of PPA. Peaks in the region 760-650 cm^{-1} region can be identified as aromatic C-H absorptions confirmed by the presence of aromatic overtones at 1750 cm^{-1} which support the presence of PPA. The split peak at 940-930 cm^{-1} identified as P-O-H characteristically appears in the 950-900 cm^{-1} region. After annealing a significant decrease in the P-O-H peak intensity is observed, as shown in Figures 5(a) and (b), indicating the reaction of a large amount of P-O-H bonds during the annealing step. Comparison of Figures 5(b) and (c) shows a further decrease in the P-O-H peak intensity and a broadening of the absorption at 950-900 cm^{-1}, attributed to removal of physi-adsorbed species during sonication. The remaining absorption is indicative of a small fraction of free P-O-H bonds, which can be attributed to a resonance structure; featuring a bidentate structure with 1 P=O and 1 P-O-H bound to the surface leaving one free P-O-H group, which has also been reported on ITO surfaces[29]. The amount of remaining P-O-H was analyzed in more detail using XPS analysis and will be discussed later in the paper. The P=O bond, usually appearing at 1250-1200 cm^{-1}, occurred at 1220 cm^{-1} as a broad peak due to the presence of hydrogen bonded species. After annealing an increase in the P=O peak intensity and a shift to

1
2
3 1180 cm^{-1} can be seen from Figures 5(a) to (b) which can be attributed to a change in
4
5 environment with P-O-H bonds becoming surface bound. ATR-FTIR analysis displays bonding
6
7
8 of PPA to the surface through P-O-H bonds by a reduction in the intensity of the absorption. The
9
10 attachment of P=O bonds cannot be distinguished by ATR-FTIR but was confirmed during XPS
11
12 analysis, as previously shown in Figure 4. Detailed characterization of the bonding mode can be
13
14
15 assessed through XPS which was used to verify and complement conclusions drawn from ATR-
16
17 FTIR by comparing the ratios of the P-O-H and P=O associated peaks in the O 1s core level.
18
19 The P=O and P-O-H components were deconvoluted and the P-O-H/O 1s and P=O/O 1s ratios
20
21
22 were used to quantify changes during the pre-anneal, post-anneal and post-sonication stages of
23
24 the process. Comparing Figures 4(a) and (b), a decrease of 30 % of the P=O component and 60
25
26 % of the P-O-H component occurred on annealing the substrate, suggesting a large proportion of
27
28
29 P-O-H bonds along with a fraction of P=O bonds reacted with the surface. ATR-FTIR analysis
30
31 did not show the clear reaction of the P=O component. However, a reduction in the P=O
32
33 component in the O 1s shows that P=O bonds also become surface bound. The O 1s spectrum
34
35
36 after rinsing the annealed sample as displayed in Figure 4(c) results in a further 30 % decrease in
37
38 P=O and P-O-H, showing that rinsing the post-anneal substrates resulted in a monolayer by
39
40 removal of physisorbed species. The remaining P=O/O 1s ratio was 30 % compared to an initial
41
42
43 physisorbed pre-anneal sample, indicative that not all P=O groups react with the substrate. A
44
45 peak associated with P-O-H bonds was not observed after sonication as most will have bonded to
46
47 the surface or be rinsed away during sonication. Therefore, a large proportion of P-O-H bonds
48
49
50 and ~60 % of P=O bonds reacted with the SiO_2 surface translating to a combination of tridentate
51
52 and bidentate attachment. Since a remaining P-O-H peak observed using ATR-FTIR can be an
53
54 indication of monodentate attachment it was investigated further as no remaining peak was found
55
56
57
58
59
60

during XPS analysis. A base rinse containing triethylamine was used to quantify the amount of unbound P-O-H. Triethylamine will coordinate to free acid groups which can be identified through the appearance of a N 1s peak using XPS[29]. No discernible N 1s peak could be identified allowing monodentate attachment to be ruled out, verifying that this peak can be attributed to a bidentate resonance structure as previously discussed. Bidentate attachment, with two P-O-H groups reacting with the surface, was confirmed due to a clear remaining P=O peak in ATR-FTIR analysis. A large decrease of the P=O component of the O1s peak is indicative of the presence of tridentate coordination which is most favorable due to the resonance stabilization when all 3 O atoms bind to the surface, which has previously been investigated on Al_2O_3 surfaces using DFT studies[31]. The binding of phosphonic acids mainly through the tridentate configuration is in agreement with literature reports[24].

1
2
3
4
5
6
7
8
9
10
11
12
13
14
15
16
17
18
19
20
21
22
23
24
25
26
27
28
29
30
31
32
33
34
35
36
37
38
39
40
41
42
43
44
45
46
47
48
49
50
51
52
53
54
55
56
57
58
59
60

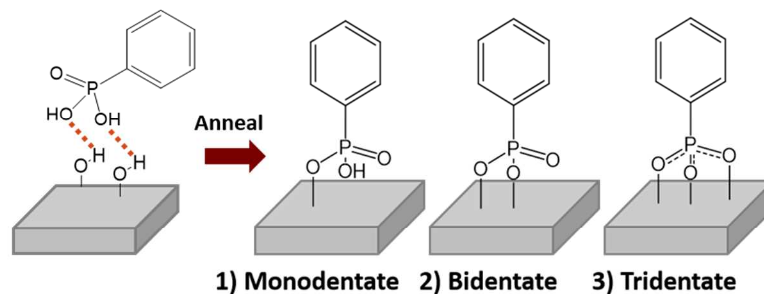

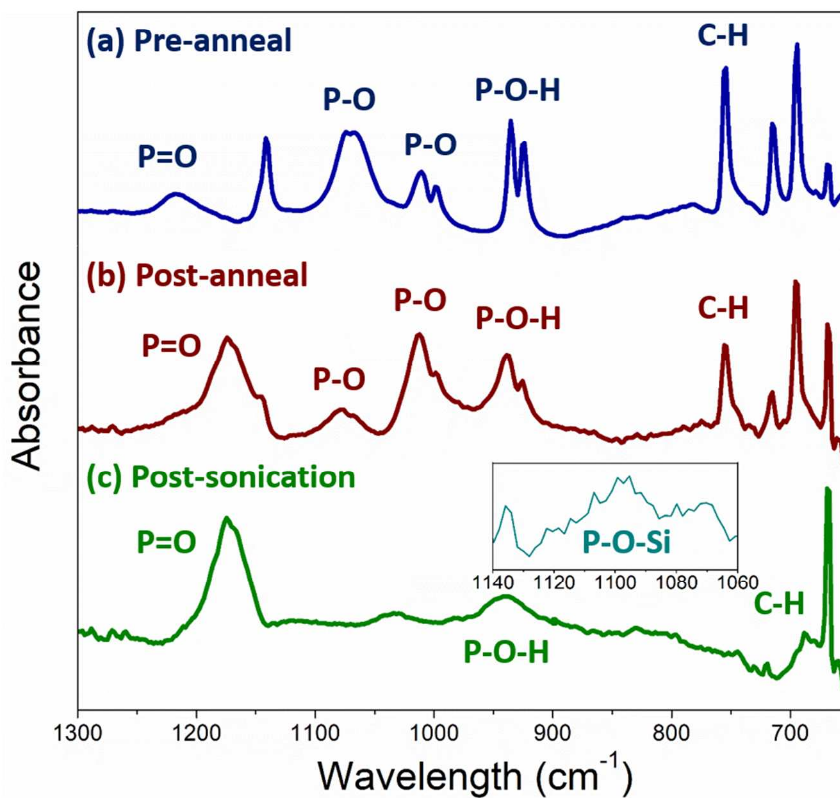

Figure 5: Surface binding mechanisms of PPA to the SiO_2 surface are displayed in (1)-(3). The surface attachment was probed using ATR-FTIR (a)-(c).

1
2
3
4
5
6
7
8
9
10
11
12
13
14
15
16
17
18
19
20
21
22
23
24
25
26
27
28
29
30
31
32
33
34
35
36
37
38
39
40
41
42
43
44
45
46
47
48
49
50
51
52
53
54
55
56
57
58
59
60

Dopant Profiling of Oxide Functionalized Surfaces

Comparison of ECV profiles of hydrosilylated and oxide functionalized Si both functionalized with VPA through 2 different strategies are shown in Figure 6(a). Similar peak carrier concentrations of 2.59×10^{20} atoms/cm^3 for hydrosilylated substrates and 2.36×10^{20} atoms/cm^3 for oxide functionalization were obtained, demonstrating oxide functionalization can be applied successfully to Si substrates without significant loss of dopant in the oxide layer.

Figure 6 (a) uses an ethanol rinse on a VPA functionalized SiO_2 surface which removes some physisorbed species to give a multilayer, however, to give complete monolayer coverage a base rinse was employed in Figure 6 (b) which subsequently results in a slightly lower peak carrier concentration. A multilayer coverage also results in a larger tail of the profile as seen by comparison of Figure 6 (a) and (b). The effect of different rinsing procedures and doping using physisorbed species is discussed later in the paper. Different sterically sized phosphonic acids were used to alter the dopant dose and investigate the effect on active carrier concentration. Figure 6(b) compares the ECV doping profiles for Si substrates where the SiO_2 surfaces were functionalized with vinyl phosphonic acid (VPA), dodecylphosphonic acid (DPA) and phenylphosphonic acid (PPA). Substrates functionalized with VPA displayed the highest peak carrier concentration at 4×10^{19} atoms/cm^3 while DPA and PPA gave peak carrier concentrations of 1×10^{19} atoms/cm^3 and 7×10^{18} atoms/cm^3, respectively. The decrease in peak carrier concentration can be attributed to different molecular packing densities of the molecules on the surface. The sterically small VPA will have the highest packing density while DPA displayed a slight decrease due to the tilt angle of the alkyl chain. A more significant decrease was observed for PPA due the sterically larger benzene ring. Additionally, the high viscosity of VPA could

permit the formation of multilayers leading to an increased dopant source and consequently, an increased carrier concentration and a slight increase of junction depth compared to PPA and DPA. The use of different sterically sized molecules has shown to influence peak carrier concentration due to the different surface coverages demonstrating that the surface functionalization step can be tailored to achieve a desired carrier concentration. Hall measurements were carried out in addition to ECV measurements to verify the accuracy of the carrier concentrations obtained. Comparison between the two techniques was carried out by calculating the dose from the ECV profiles and comparing it to the dose obtained through Hall measurements. A dose of 3×10^{13} atoms/cm^2 was obtained for VPA using Hall measurements, comparable to 1.5×10^{14} atoms/cm^2 determined by ECV measurements. Substrates doped using PPA also displayed good agreement, with values of 1.2×10^{13} atoms/cm^2 obtained for Hall and 1.9×10^{13} atoms/cm^2 obtained for ECV. Mobility values of 217 and 129 cm^2/Vs were obtained for PPA and VPA.

The RTA temperature also influences the doping profile, with lower temperatures resulting in a shallower doping profile but also giving a lower carrier concentration. A range of annealing temperatures between 950-1100 ºC were investigated to find the optimum RTA temperature when doping SiO_2 functionalized substrates. The highest peak carrier concentration of 7.87×10^{19} atoms/cm^3 was obtained at an RTA temperature of 1000 °C as shown in Figure S5 (see Supporting Information). In comparison the optimal RTA temperature reported for conventional MLD using hydrosilylation was 1050 ºC[3]. Higher annealing temperatures of 1100 °C displayed a slight decrease in active carrier concentration to 3.09×10^{19} atoms/cm^3 with an increase in junction depth to 100 nm taken at 1.36×10^{18} atoms/cm^3. Substrates annealed at 950 °C

1
2
3
4
5
6
7
8
9
10
11
12
13
14
15
16
17
18
19
20
21
22
23
24
25
26
27
28
29
30
31
32
33
34
35
36
37
38
39
40
41
42
43
44
45
46
47
48
49
50
51
52
53
54
55
56
57
58
59
60

displayed a decrease in junction depth to 22 nm at 1.72×10^{18} atoms/cm^3. Substrates annealed at 750 °C and 850 °C were also investigated, however no doping was observed at these temperatures suggesting the temperature was not high enough to allow significant dopant diffusion. The effect of RTA temperature was in agreement with the literature,[1] with a temperature of 950 °C reducing junction depth and a temperature of 1000 °C giving the maximum carrier concentration for oxide-MLD. In order to obtain a higher peak carrier concentration without modifying temperature, the effect of adding a larger concentration of dopant source, by using a physisorbed layer, was investigated. Physisorbed samples were prepared using the oxide functionalization procedure but samples were not subjected to rinsing, leaving a physisorbed overlayer which was used as a dopant source. The ECV profiles in Figure S6 (see Supporting Information) illustrate an increase in peak carrier concentration from 5.74×10^{18} atoms/cm^3 to 2.36×10^{19} atoms/cm^3 for substrates doped using physisorbed PPA compared to chemisorbed PPA, due to the presence of a thicker layer of dopant. Physisorbed samples demonstrated less reproducibility compared to chemisorbed samples. The chemisorbed monolayer provides a fixed amount of dopant source each time due to the monolayer coverage obtained using a rinse after the annealing step. Less control can be achieved when preparing physisorbed samples due to non-uniformity in the thickness of the overlayer leading to variations in the amount of dopant source accounting for the differences in peak carrier concentration. VPA functionalized substrates showed very similar peak carrier concentrations for chemisorbed (3.42×10^{19} atoms/cm^3) and physisorbed (4.39×10^{19} atoms/cm^3) substrates. VPA had an extremely high viscosity and complete removal of physisorbed species was difficult even under prolonged sonication. Different rinsing procedures were employed to remove as much physisorbed species as possible from chemisorbed substrates. An ethanol rinse, 10 min

sonication in THF followed by 10 min in ethanol, was used initially and compared to a base rinse, 10 min sonication in an aqueous trimethylamine mixture followed by 10 min in ethanol. A base rinse (3.42×10^{19} atoms/cm^3) was found to be most efficient in removal of physisorbed material for VPA functionalized substrates compared to an ethanol rinse (2.24×10^{20} atoms/cm^3). Substrates functionalized with PPA and DPA showed similar profiles for both rinses indicating that the ethanol rinse sufficiently removed physisorbed species. A more important effect observed for physisorbed samples was the increase in junction depth associated with all three molecules, especially VPA, as shown in Figure S6 (see Supporting Information). The physisorbed layer provides a larger concentration of dopant source which increases the tail of the profile as shown in Figure S6 rather than resulting in significantly higher peak carrier concentrations. Ye *et al.* [7] demonstrated that increasing the boron monolayer content on the Si surface lead to an increase in junction depth instead of an increase in peak carrier concentration and the thermal budget proved to be more effective than the dopant source in tailoring the dopant profile, in agreement with our results. Therefore, the functionalization of SiO_2 overlayers on Si is more effective in obtaining shallow profiles in Si while maintaining comparably high peak carrier concentrations.

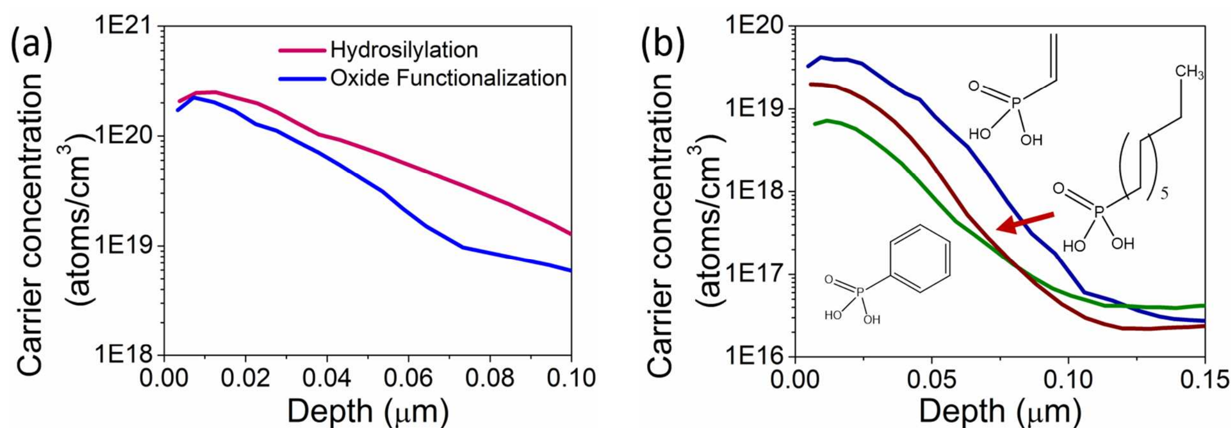

Figure 6: (a) ECV profiles comparing hydrosilylated and oxide functionalized Si surfaces using VPA. (b) ECV profiles comparing oxide functionalization using different phosphonic acids: VPA (top), DPA (middle), PPA (bottom).

Applications of Oxide-MLD

Lower RTA temperatures have previously been used to reduce junction depth which are accompanied by a reduction in carrier concentration[1]. To reduce junction depth while maintaining comparable peak carrier concentrations, the thickness of the SiO_2 overlayer was varied to slow diffusion during the RTA process. The SiO_2 was grown chemically and electrochemically on Si using previously published procedures[21, 22] and the influence on peak carrier concentration and junction depth is displayed in Figure 7. In preliminary tests, an electrochemically grown oxide thickness of 5 nm was found to result in a reduction in carrier concentration, also leading to a reduction in junction depth from 40 nm at 1.08×10^{18} atoms/cm^3 to 26 nm at 1.19×10^{18} atoms/cm^3. The effect was minimal as a reduction in peak carrier concentration was also observed. Since electrochemically grown oxide layers can have a lower

density then thermally grown oxides[32], a thicker layer of 10 and 20 nm was grown which resulted in a reduction in junction depth from 45 nm at 1.31×10^{18} atoms/cm^3 to 19 nm at 1.58×10^{18} atoms/cm^3 for a 20 nm oxide layer, while maintaining a high peak carrier concentration of 4.65×10^{18} atoms/cm^3. The reduction in junction depth is displayed in Figure 7(b). Chemically grown SiO_2 overlayers on Si were also prepared which typically have higher densities than electrochemically grown oxides[32]. Figure 7(a) shows the ECV profile of a Si substrate with a 5.2 nm SiO_2 layer, chemically grown using the NAOS procedure[21,22]. Chemically grown oxides showed a similar effect to electrochemical oxides with a reduction in junction depth from 45 nm at 1.31×10^{18} atoms/cm^3 to 29 nm at 1.31×10^{18} atoms/cm^3. While this result is indicative that the oxide layer thickness can be used to modify junction depth in Si substrates, further work to optimize the chemical and electrochemical growth is required.

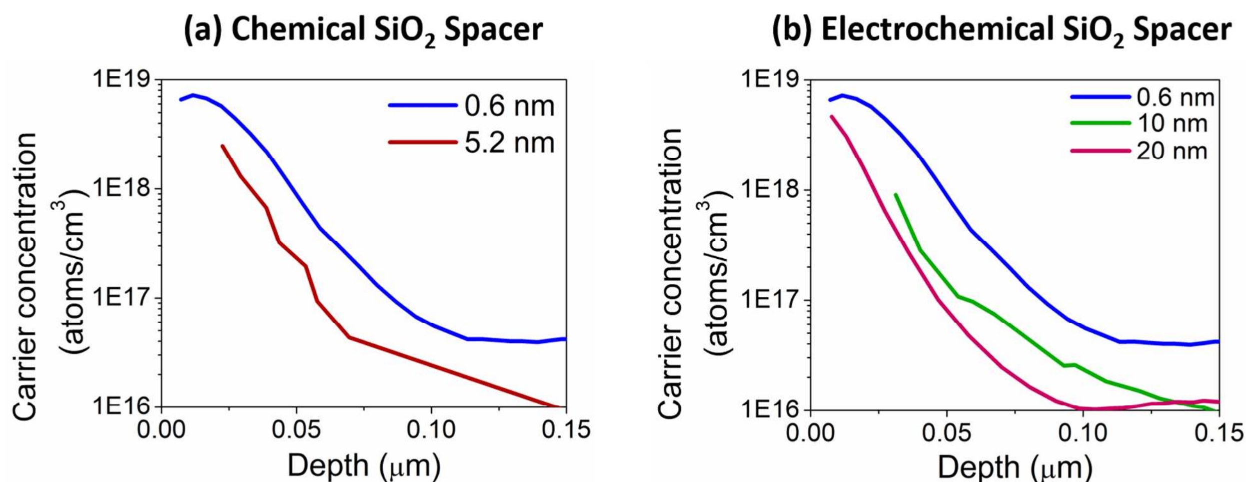

Figure 7: ECV doping profiles of Si obtained using (a) a chemically and (b) electrochemically grown oxide spacer.

1 2 3 4 5 6 7 8 9 10 11 12 13 14 15 16 17 18 19 20 21 22 23 24 25 26 27 28 29 30 31 32 33 34 35 36 37 38 39 40 41 42 43 44 45 46 47 48 49 50 51 52 53 54 55 56 57 58 59 60

Functionalization of the surface oxide on Si also enables a large range of doping precursors to be selected. Oxide-MLD can be applied to p-doping using boron precursors with successful attachment of boric acid (BA) and phenylboronic acid (PBA), as confirmed using XPS. The spectrum shown in Figure S7 (see Supporting Information) was acquired at an angle of 75 ° and displays the B 1s peak at 190 eV, demonstrating successful attachment of boron precursors allowing this strategy to be applied to p-doping. A further advantage of using BA as the dopant source is the absence of carbon in the molecule thereby preventing carbon contamination which is a major issue arising from doping semiconductor substrates using the MLD process[33]. Theoretical studies on oxide-MLD have reported the release of the carbon ligand before phosphorus enters the substrate hence eliminating the need for a capping layer[33]. Substrates that were subjected to MLD without a capping layer were found to be have an extremely high contact resistance, making extraction of a doping profile impossible and indicating low doping levels. The use of a capping layer was found to be essential in obtaining reproducible results. While work has been done to eliminate carbon contamination in the form of self-capping precursors[14, 15], we have demonstrated the attachment of carbon-free precursors which will ensure a carbon-free substrate. MLD often involves hydrosilylation reactions since precursors are chosen based on their alkene functionality which facilitates attachment of the dopant molecule, however these precursors can result in carbon contamination after the RTA. Carbon contamination also arises from adventitious hydrocarbons which can diffuse into the Si during annealing. Oxide functionalization allows the option of selecting carbon-free precursors, as attachment occurs through the phosphonic acid head group with surface silanol groups on the SiO_2 overlayer of the Si substrate. We have demonstrated successful doping using a carbon-free precursor, phosphorus pentoxide (P_2O_5), as shown in Figure 8(a). An increase in P_2O_5 concentration was

1
2
3
4
5
6
7
8
9
10
11
12
13
14
15
16
17
18
19
20
21
22
23
24
25
26
27
28
29
30
31
32
33
34
35
36
37
38
39
40
41
42
43
44
45
46
47
48
49
50
51
52
53
54
55
56
57
58
59
60

found to result in higher carrier concentrations demonstrating the potential for tuning the carrier concentration using chemical functionalization of the surface.

Additionally, the SiO_2 overlayer can act as a barrier to contamination by trapping impurities that may otherwise diffuse into Si in conventional MLD. Carbon has been reported to segregate at the SiO_2-Si interface but remain on the SiO_2 side[19]. The oxide layer is removed using HF treatment after the MLD process hence ensuring a carbon-free substrate. SIMS studies have confirmed carbon remains in the SiO_2 layer when substrates are subjected to carbon implants[19]. SIMS analysis displayed in Figure 8(b) shows an increase in carbon concentration at the SiO_2-Si interface, with the peak concentration occurring on the SiO_2 side of the interface. The P doping profile correlates well with ECV analysis with only a minor increase in concentration, suggesting the presence of a high amount of electrically active dopants. The carbon concentration in oxide-MLD doped substrates does not exceed the levels of carbon observed in a reference Si substrate ($\sim 1 \times 10^{18}$ atoms/cm^3) displayed in Figure S8 (see Supporting Information). Low carbon levels are in corroboration with the low mobility value of 217 cm^2/Vs obtained using Hall measurements for a PPA doped substrate which can give an indication of the level of carbon contamination. Carbon diffusion has been reported to be limited to the first few monolayers[34] but the use of an oxide overlayer creates a robust barrier to carbon diffusion that can be removed after RTA, suggesting it is an effective method of eliminating carbon contamination.

1
2
3
4
5
6
7
8
9
10
11
12
13
14
15
16
17
18
19
20
21
22
23
24
25
26
27
28
29
30
31
32
33
34
35
36
37
38
39
40
41
42
43
44
45
46
47
48
49
50
51
52
53
54
55
56
57
58
59
60

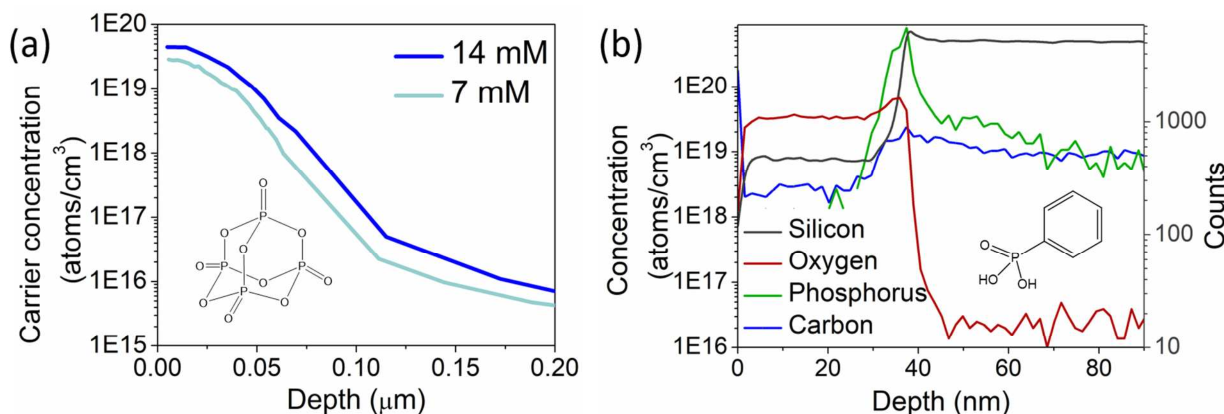

Figure 8: (a) ECV profiles of phosphorus pentoxide, a carbon-free precursor. (b) SIMS profile after RTA of a 50 nm SiO_2 capped Si substrate functionalized with PPA showing Si, O, C and P profiles.

Conclusions

The functionalization of SiO_2 surfaces has proven to be a more successful strategy of doping Si compared to hydrosilylation reactions when attaching precursors for MLD. Improved stability was observed without the need for purification and inert conditions. Successful application of the oxide-MLD strategy to both p- and n-doping was demonstrated. Comparable peak carrier concentrations were achieved for both strategies and the effect of using a physisorbed overlayer was found to result in similar peak carrier concentrations but significantly larger junction depths. This method allows carbon contamination to be minimized through the selection of carbon-free precursors, while the use of an oxide layer which traps carbon at the interface will minimize carbon in the doped substrate if carbon containing precursors are used. Tuning the thickness of the SiO_2 overlayer can be used to influence junction depth, however further work is required to optimize this strategy. Oxide-MLD has demonstrated to be a versatile method of doping Si surfaces resulting in minimal carbon contamination. In addition to planar Si surfaces, the mild

processing conductions used for oxide-MLD is particularly advantageous for doping Si nanostructures such as nanowires where controlled functionalization of the surface is required.

Supporting Information

Further characterization including XPS spectra, WCA measurements, ECV and SIMS analysis of functionalized and doped Si substrates. Supporting information is available free of charge on the ACS Publications website

Acknowledgements

This work was funded by the Irish Research Council Government of Ireland Postgraduate Scholarship Programme under grant number GOIPG/2015/2933. The authors would like to thank Jean-Paul Barnes for SIMS analysis funded by the European Union Horizon 2020 research and innovation programme (grant agreement number 654384) under the ASCENT programme (project reference 070). The authors would also like to thank Dr Pietro Pampili for carrying out Hall measurements.

1
2
3
4
5
6
7
8
9
10
11
12
13
14
15
16
17
18
19
20
21
22
23
24
25
26
27
28
29
30
31
32
33
34
35
36
37
38
39
40
41
42
43
44
45
46
47
48
49
50
51
52
53
54
55
56
57
58
59
60

References

(1) Ho, J. C.; Yerushalmi, R.; Jacobson, Z. a; Fan, Z.; Alley, R. L.; Javey, A. Controlled Nanoscale Doping of Semiconductors via Molecular Monolayers. *Nat. Mater.* **2008**, *7* (1), 62–67.

(2) Purser, K. H.; Farrell, J. P. *Ion Implantation Science and Technology*; Elsevier, 1984.

(3) O'Connell, J.; Verni, G. A.; Gangnaik, A.; Shayesteh, M.; Long, B.; Georgiev, Y. M.; Petkov, N.; McGlacken, G. P.; Morris, M. A.; Duffy, R.; Holmes, J. D. Organo-Arsenic Molecular Layers on Silicon for High-Density Doping. *ACS Appl. Mater. Interfaces* **2015**, *7* (28), 15514–15521.

(4) Veerbeek, J.; Ye, L.; Vijselaar, W.; Kudernac, T.; van der Wiel, W. G.; Huskens, J. Highly Doped Silicon Nanowires by Monolayer Doping. *Nanoscale* **2017**, *9* (8), 2836–2844.

(5) O'Connell, J.; Napolitani, E.; Impellizzeri, G.; Glynn, C.; McGlacken, G. P.; O'Dwyer, C.; Duffy, R.; Holmes, J. D. Liquid-Phase Monolayer Doping of InGaAs with Si-, S-, and Sn-Containing Organic Molecular Layers. *ACS Omega* **2017**, *2* (5), 1750–1759.

(6) Long, B.; Alessio Verni, G.; O'Connell, J.; Holmes, J.; Shayesteh, M.; O'Connell, D.; Duffy, R. Molecular Layer Doping: Non-Destructive Doping of Silicon and Germanium. In *2014 20th International Conference on Ion Implantation Technology (IIT)*; Portland, 2014; pp 1–4.

(7) Ye, L.; González-Campo, A.; Nuñez, R.; de Jong, M. P.; Kudernac, T.; van der Wiel, W. G.; Huskens, J. Boosting the Boron Dopant Level in Monolayer Doping by Carboranes. *ACS Appl. Mater. Interfaces* **2015**, 7 (49), 27357-27361.

(8) Wu, H.; Guan, B.; Sun, Y.; Zhu, Y.; Dan, Y. Controlled Doping by Self-Assembled

Dendrimer-like Macromolecules. *Sci. Rep.* **2017**, *7*, 41299.

(9) Voorthuijzen, W. P.; Yilmaz, M. D.; Naber, W. J. M.; Huskens, J.; van der Wiel, W. G. Local Doping of Silicon Using Nanoimprint Lithography and Molecular Monolayers. *Adv. Mater.* **2011**, *23* (11), 1346–1350.

(10) Ho, J. C.; Yerushalmi, R.; Smith, G.; Majhi, P.; Bennett, J.; Halim, J.; Faifer, V. N.; Javey, A. Wafer-Scale, Sub-5 Nm Junction Formation by Monolayer Doping and Conventional Spike Annealing. *Nano Lett.* **2009**, *9* (2), 725–730.

(11) O'Connell, J.; Biswas, S.; Duffy, R.; Holmes, J. D. Chemical Approaches for Doping Nanodevice Architectures. *Nanotechnology* **2016**, *27* (34), 342002.

(12) Bent, S. F. Organic Functionalization of Group IV Semiconductor Surfaces: Principles, Examples, Applications, and Prospects. *Surf. Sci.* **2002**, *500* (1–3), 879–903.

(13) Collins, G.; O'Dwyer, C.; Morris, M.; Holmes, J. D. Palladium-Catalyzed Coupling Reactions for the Functionalization of Si Surfaces: Superior Stability of Alkenyl Monolayers. *Langmuir* **2013**, *29* (38), 11950–11958.

(14) Mathey, L.; Alphazan, T.; Valla, M.; Veyre, L.; Fontaine, H.; Enyedi, V.; Yckache, K.; Danielou, M.; Kerdiles, S.; Guerrero, J.; Barnes, J.-P.; Veillerot, M.; Chevalier, N.; Mariolle, D.; Bertin, F.; Durand, C.; Berthe, M.; Dendooven, J.; Martin, F.; Thieuleux, C.; Grandidier, B.; Copéret, C. Functionalization of Silica Nanoparticles and Native Silicon Oxide with Tailored Boron-Molecular Precursors for Efficient and Predictive P -Doping of Silicon. *J. Phys. Chem. C* **2015**, *119* (24), 13750–13757.

(15) Alphazan, T.; Mathey, L.; Schwarzwälder, M.; Lin, T.-H.; Rossini, A. J.; Wischert, R.; Enyedi, V.; Fontaine, H.; Veillerot, M.; Lesage, A.; Emsley, L.; Veyre, L.; Martin, F.; Thieuleux, C.; Copéret, C. Monolayer Doping of Silicon through Grafting a Tailored

1
2
3
4
5
6
7
8
9
10
11
12
13
14
15
16
17
18
19
20
21
22
23
24
25
26
27
28
29
30
31
32
33
34
35
36
37
38
39
40
41
42
43
44
45
46
47
48
49
50
51
52
53
54
55
56
57
58
59
60

Molecular Phosphorus Precursor onto Oxide-Passivated Silicon Surfaces. *Chem. Mater.* **2016**, 28 (11), 3634-3640.

(16) Pujari, S. P.; Scheres, L.; Marcelis, A. T. M.; Zuilhof, H. Covalent Surface Modification of Oxide Surfaces. *Angew. Chemie Int. Ed.* **2014**, *53* (25), 6322–6356.

(17) Vega, A.; Thissen, P.; Chabal, Y. J. Environment-Controlled Tethering by Aggregation and Growth of Phosphonic Acid Monolayers on Silicon Oxide. *Langmuir* **2012**, *28* (21), 8046–8051.

(18) Thissen, P.; Seitz, O.; Chabal, Y. J. Wet Chemical Surface Functionalization of Oxide-Free Silicon. *Prog. Surf. Sci.* **2012**, *87* (9–12), 272–290.

(19) Ichiro, M.; Eiji, K.; Norihisa, A.; Masahisa, S.; Masahiko, Y.; Shin-ichi, T.; Mikio, W.; Shigeru, K.; Yuichi, M.; Sei-ichi, M.; Masahiro, K. Diffusion and Segregation of Carbon in SiO2 Films. *Jpn. J. Appl. Phys.* **1997**, *36* (3S), 1465.

(20) Hoarfrost, M. L.; Takei, K.; Ho, V.; Heitsch, A.; Trefonas, P.; Javey, A.; Segalman, R. A. Spin-On Organic Polymer Dopants for Silicon. *J. Phys. Chem. Lett.* **2013**, *4* (21), 3741–3746.

(21) S. Imai, M. Takahashi, K. Matsuba, Asuha, Y. Ishikawa, H. Kobayashi, S. Formation and Electrical Characteristics of Silicon Dioxide Layers by Use of Nitric Acid Oxidation Method. *Acta Phys. slovaca* **2005**, *55* (3), 305–313.

(22) Asuha; Im, S.-S.; Tanaka, M.; Imai, S.; Takahashi, M.; Kobayashi, H. Formation of 10–30nm SiO2/Si Structure with a Uniform Thickness at ~120°C by Nitric Acid Oxidation Method. *Surf. Sci.* **2006**, *600* (12), 2523–2527.

(23) Cumpson, P. J.; Zalm, P. C. Thickogram: A Method for Easy Film Thickness Measurement in XPS. *Surf. Interface Anal.* **2000**, *29*, 403–406.

1
2
3
4
5
6
7
8
9
10
11
12
13
14
15
16
17
18
19
20
21
22
23
24
25
26
27
28
29
30
31
32
33
34
35
36
37
38
39
40
41
42
43
44
45
46
47
48
49
50
51
52
53
54
55
56
57
58
59
60

(24) Gouzman, I.; Dubey, M.; Carolus, M. D.; Schwartz, J.; Bernasek, S. L. Monolayer vs. Multilayer Self-Assembled Alkylphosphonate Films: X-Ray Photoelectron Spectroscopy Studies. *Surf. Sci.* **2006**, *600* (4), 773–781.

(25) Yerushalmi, R.; Ho, J. C.; Fan, Z.; Javey, A. Phosphine Oxide Monolayers on SiO2 Surfaces. *Angew. Chem. Int. Ed. Engl.* **2008**, *47* (23), 4440–4442.

(26) Branch, B.; Dubey, M.; Anderson, A. S.; Artyushkova, K.; Baldwin, J. K.; Petsev, D.; Dattelbaum, A. M. Investigating Phosphonate Monolayer Stability on ALD Oxide Surfaces. *Appl. Surf. Sci.* **2014**, *288*, 98–108.

(27) Dubey, M.; Weidner, T.; Gamble, L. J.; Castner, D. G. Structure and Order of Phosphonic Acid-Based Self-Assembled Monolayers on Si(100). *Langmuir* **2010**, *26* (18), 14747–14754.

(28) Hanson, E. L.; Schwartz, J.; Nickel, B.; Koch, N.; Danisman, M. F. Bonding Self-Assembled, Compact Organophosphonate Monolayers to the Native Oxide Surface of Silicon. *J. Am. Chem. Soc.* **2003**, *125* (51), 16074–16080.

(29) Paniagua, S. a; Hotchkiss, P. J.; Jones, S. C.; Marder, S. R.; Mudalige, A.; Marrikar, F. S.; Pemberton, J. E.; Armstrong, N. R. Phosphonic Acid Modification of ITO Electrodes - Combined XPS - UPS - Contact Angle Studies. *J. Phys. Chem. C* **2008**, *112* (21), 7809–7817.

(30) Thissen, P.; Vega, A.; Peixoto, T.; Chabal, Y. J. Controlled, Low-Coverage Metal Oxide Activation of Silicon for Organic Functionalization: Unraveling the Phosphonate Bond. *Langmuir* **2012**, *28* (50), 17494–17505.

(31) Hector, L. G.; Opalka, S. M.; Nitowski, G. A.; Wieserman, L.; Siegel, D. J.; Yu, H.; Adams, J. B. Investigation of Vinyl Phosphonic Acid/hydroxylated -Al2O3(0001)

1
2
3
4
5
6
7
8
9
10
11
12
13
14
15
16
17
18
19
20
21
22
23
24
25
26
27
28
29
30
31
32
33
34
35
36
37
38
39
40
41
42
43
44
45
46
47
48
49
50
51
52
53
54
55
56
57
58
59
60

Reaction Enthalpies. *Surf. Sci.* **2001**, *494* (1), 1–20.

(32) Philipsen, H. G. G.; Kelly, J. J. Anisotropy in the Anodic Oxidation of Silicon in KOH Solution. *J. Phys. Chem. B* **2005**, *109* (36), 17245–17253.

(33) Longo, R. C.; Cho, K.; Schmidt, W. G.; Chabal, Y. J.; Thissen, P. Monolayer Doping via Phosphonic Acid Grafting on Silicon: Microscopic Insight from Infrared Spectroscopy and Density Functional Theory Calculations. *Adv. Funct. Mater.* **2013**, *23* (27), 3471–3477.

(34) Shimizu, Y.; Takamizawa, H.; Inoue, K.; Yano, F.; Nagai, Y.; Lamagna, L.; Mazzeo, G.; Perego, M.; Prati, E. Behavior of Phosphorous and Contaminants from Molecular Doping Combined with a Conventional Spike Annealing Method. *Nanoscale* **2014**, *6* (2), 706–710.

1
2
3
4
5
6
7
8
9
10
11
12
13
14
15
16
17
18
19
20
21
22
23
24
25
26
27
28
29
30
31
32
33
34
35
36
37
38
39
40
41
42
43
44
45
46
47
48
49
50
51
52
53
54
55
56
57
58
59
60

Table of Contents Figure